A Relaxation Method for Surface-Conforming Prisms

Ross Whitaker, Robert M. Kirby, Zhisong Fu
Scientific Computing and Imaging Institute, University of Utah
Salt Lake City, UT 84112

Abstract:
This paper presents a method for computing thin layers of high-quality, triangular prisms that conform to surfaces that are specified as level sets of an implicit function. Triangular prisms are important in circumstances where volumetric meshes need to capture the geometries materials with thin layers–*i.e.* that are smooth relative to their thickness–or where, as in fluid mechanics simulations, solutions perpendicular to boundaries exhibit boundary layer complexities that exceed that of the bounding surfaces. "High-quality" triangular prisms exhibit a roughly linear structure, with nearly regular triangles at the ends and side faces that are nearly perpendicular to the triangular faces. The proposed method relies on an iterative relaxation of point samples, which we call *dynamic particles*, that simultaneously regularize inter-point distance on the surfaces while shortening distances to corresponding points on a nearby offset surface, which establishes the layer. This paper describes the method and results on meshes of medical data sets that model human vasculature.

1 Introduction

This paper presents a method for computing thin layers of high-quality, triangular prisms that conform to surfaces that are specified as level sets of an implicit function. This problem statement is motivated by a number of applications in medicine and biology where simulations are conducted on geometric models derived from 3D images, such as CT, MRI, or various forms of microscopy. These applications, in fields such as electrophysiology [4], orthopedics, and cardiology [3], rely on a wide range of governing equations, such as electrostatics, fluid dynamics, solid mechanics, and chemical dynamics. Here we consider three particular driving problems: electrostatic simulations in the head for EEG, in which thin layers around the skin and skull present thin, layered geometries; hyperelastic simulations of mouse bone loading where stress boundary layers normal to the surface must be captured; and computational fluid dynamics of human vasculature, where meshes of complex, branching structures must be augmented with thin layers to capture the properties of fluid flow near boundaries. In this paper we present meshing results for the latter.

Figure 1(a)–(b) shows an example of a segmentation from head MRI that demonstrates the thin layers of tissue which can have very different electrical conductivity—an important consideration in the simulation of biolelectric fields. Figure 1(c)–(d) shows a segmentation and an adaptive mesh of a rela-

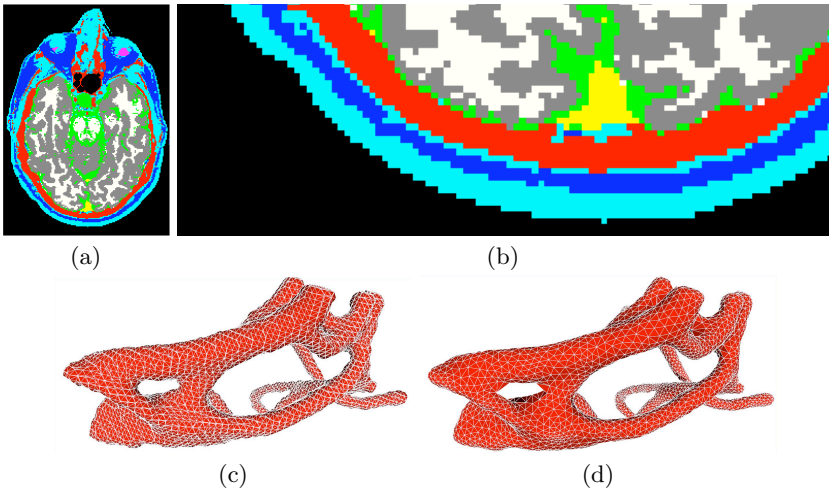

Fig. 1: (a)–(b) Segmentations of MRI head data show thin layers of skin, skull, fat and cerebral spinal fluid. (c) Isosurfaces of CT angiography give boundaries of vascular lumen, where blood flows. (d) Adaptive meshes using the method of dynamic particles [2] give good quality triangles and watertight surfaces.

tively small section of a CT data set from a human head. Fluid simulations rely on thin elements near the vessel boundaries to capture high gradients in flow.

One typical strategy for constructing such prisms is to start with a good quality triangle surface and simply offset the triangle vertices in the direction of the surface normals (established from the adjacent triangles, *e.g.* an average), and build prisms from the set of resulting triangle pairs. The first problem with this is that the prisms may not be valid. Here we define *validity* as nonself-intersecting prisms—that represent a single, connected solid. For instance, in regions of high curvature, the offsets that form the uprights of the prisms can cross the quadrilateral faces. The second problem is that even if the prisms are valid, the *quality* of the prisms could be compromised with this approach. This is because surface normals for each vertex are not parallel and because the inner and out triangular faces are not parallel. This can change the shape of the individual triangles and cause uprights that are skewed relative to the faces.

Figure 2a shows quantitative results of this strategy. For triangle quality we use the radius ratio: $Q = 3r/R$, where r and R are the radii of inscribing and circumscribing circles, respectively. This figure shows the effect of the offset on Q, as represented by histograms, which is quite good for the original triangle mesh (Fig. 2a—blue), but degrades significantly in the offset (Fig. 2a—red). The average radius ratio drops from 0.92 to 0.72. The angles between the quadrilateral faces and the triangles is $A = \text{asin}(\mathbf{u} \cdot \mathbf{n})$, where $\mathbf{u}$ is the unit vector along the quadrilateral edge, and $\mathbf{n}$ is the unit surface normal. Ideally,

this would be 90 degrees. The average angle is 74 degrees and the minimum is 0.2 degrees—there are some very skewed prisms. Finally, the number of incorrect prisms is significant—160 out of 11,854 prisms are of poor quality (1.3%) and would need to be corrected either by direct user interaction or some other mechanism. The purpose of this paper is to examine an alternative to this simple approach.

2 Methods

The meshing method uses a set of points, which we call *particles* [5, 1], whose positions are updated along the gradient of an objective function that prefers regular configurations. In previous work, we have shown that these objective functions can be constructed to achieve adaptive, high-quality sampling of implicit surfaces [2]. The objective function is a sum of local potential functions of the form $E(r_{ij}) \sim \mathrm{cotan}(\mathrm{r_{ij}}/\alpha)$, where r_{ij} is the distance between points (particles) i and j, $r_{ij} = |\mathbf{x}_i = \mathbf{x}_j|$. The total energy, for N particles is $P = \sum_{i=1}^{N} \sum_{j \neq i} E(r_{ij})$. The derivative of this energy (Figure 2c) is compact, and particles move with a gradient descent on this potential, constrained to the isosurface $V(\mathbf{x}) = k$.

For prisms, we establish a set of corresponding particles, with potential $P' = \sum_{i'=1}^{N} \sum_{j' \neq i'} E(r_{i'j'})$. These particles are constrained to an alternative isosurface $V(\mathbf{x}) = k'$, and we obtain an ϵ offset if $k' = k + \epsilon$ and $V(\mathbf{x})$ is a distance function to the original surface. Finally the two systems of particles are coupled, in order to keep correspondences close, through a quadratic energy, $S_i = |x_i - x'_i|^2$, and we have

$$R = P + P' + \alpha \sum_{i=1}^{N} S_i, \tag{1}$$

as depicted in Figure 2b.

To initialize, we use the *simple* method described above, where we first optimize on the original surface, place twin particles on the offset surface, and then optimize the joint energy in Equation 1, which optimizes the particles on the two surface while keeping corresponding particles close. For all the results in this paper we use $\alpha = 10$. As in previous work [2], we insert and remove particles so that each particle (on the original surface) has a distance to its neighbors that is to within a specified tolerance of the local feature size. The local feature size is determined by measuring both the surface curvature and the distance to the medial axis.

3 Results and Conclusions

We begin with a simple geometric structure, which is a metacarpal of a mouse (finger/paw bone). Figure 3 shows a particle distribution from the proposed

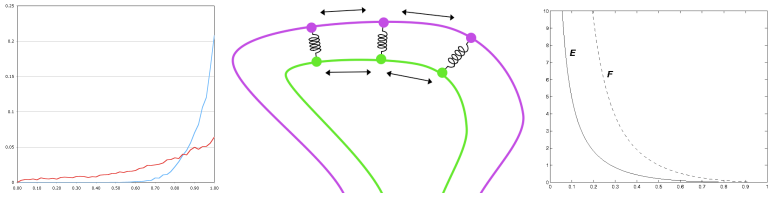

(a) (b) (c)

Fig. 2: (a) Histograms of radius ratios of the original surface and offset (blue and red respectively), show a degradation of the triangle quality in the offset surface (Radius ratio of 1.0 is ideal). (b) Particles on each surface, the original and the offset, repel each other to maintain good configurations, but are attracted to the corresponding particle on the other surface. (c) The potential energy and repulsive force between particles falls off as *cotan*, approximating an electrostatic potential, but with compact support.

method and the resulting mesh. Table 3 summarizes the quantitative results. The proposed mesh eliminates the five poor quality prisms, improves the average and minimum radius ratios, but introduces slightly more *skew* in the prisms, as indicated by the average and maximum prism angles. Figure 3 shows the prism mesh of the vessel data. The quantitative results in Table 3 demonstrate an overall improvement but not the ideal results. The number of poor quality elements drops by 75% (160 to 40), and the triangles improve, but not entirely.

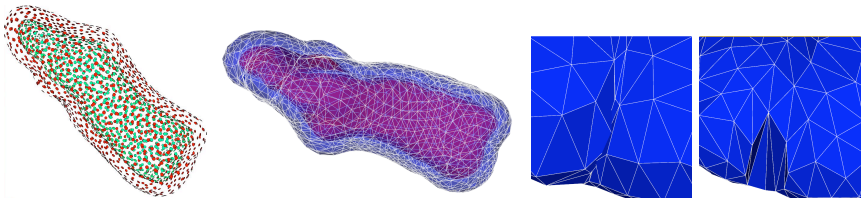

(a) (b) (c) (d)

Fig. 3: (a) Distribution of points/particles on a single surface—red and green are original and offset surfaces, respectively. (b) Prisms from the proposed method. (c) Offset surface from the *simple* method (normal offsets), show invalid (intersecting) elements. (d) Same view as (c) for the proposed method—showing valid prisms.

The results, therefore, are promising but mixed. In the case of invalid prisms, one can show that such prisms must always come in pairs, and that the energy of the system must be improved by swapping vertices. This suggests that the problem is the minimization, which is certainly getting trapped in local minima. Also, the parameters themselves—the tradeoff between particle repulsion and particle attraction—needs further attention. Another issue is that we use a DT triangulation method on the initial surface, and let the offset surface inherit this triangulation from the correspondences. We have noticed

that the triangles are consistently better on the initial surface, suggesting the need for a more holistic approach for the final meshing phase of the algorithm. Also, the offsets in these results are large relative to the surface geometry, which is intentional so that we could examine the behavior of the system as it fails. For the future, the integration of this system with the construction of multiple, thinner prismatic layers and tetrahedral volumes could help with the overall quality and allow better testing of performance.

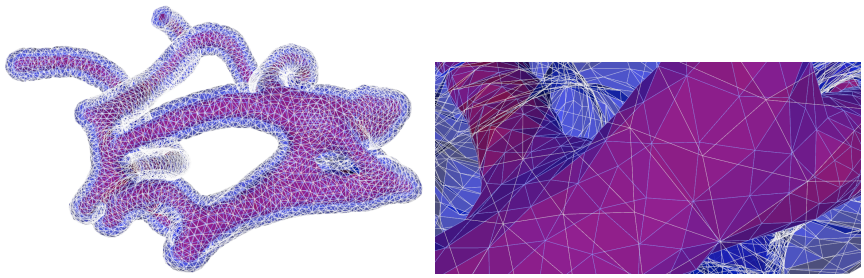

Method	Rad Ratio Avg	Rad Ratio Min	Angle Avg	Angle Min	Invalid Elements
Mouse Bone					
Simple	0.87	3.0×10^{-2}	79.8	2.1×10^{-1}	5
Particle	0.88	7.2×10^{-2}	67.5	7.2×10^{-2}	0
Vessels					
Simple	0.82	4.9×10^{-4}	72.7	2.1×10^{-2}	160
Particle	0.83	4.0×10^{-3}	74.4	9.7×10^{-2}	40

References

1. M. Meyer, P. Georgel, and R. Whitaker. Robust particle systems for curvature dependent sampling of implicit surfaces. In *Proceedings of the International Conference on Shape Modeling and Applications (SMI)*, pages 124–133, June 2005.
2. M. Meyer, R. M. Kirby, and R. Whitaker. Topology, accuracy, and quality of isosurface meshes using dynamic particles. *IEEE Transactions on Visualization and Computer Graphics*, 12(5):1704–1711, September/October 2007.
3. C. A. Taylor and M. T. Draney. Experimental and computational methods in cardiovascular fluid mechanics. *Annual Review of Fluid Mechanics*, 36:197–231, 2004.
4. R. V. Uitert, C. Johnson, and L. Zhukov. Influence of head tissue conductivity in forward and inverse magnetoencephalographic simulations using realistic head models. *IEEE Transactions on Biomedical Engineering*, 51(12):2129–2137, 2004.
5. A. P. Witkin and P. S. Heckbert. Using particles to sample and control implicit surfaces. In *Proceedings of the 21st annual conference on Computer graphics and interactive techniques*, pages 269–277. ACM Press, 1994.